DEVELOPMENT OF A GAS SHEET BEAM PROFILE MONITOR FOR IOTA[*]

S. Szustkowski[†1], S. Chattopadhyay[1,2], D. Crawford[2], B. Freemire[1]
[1]Northern Illinois University, DeKalb, IL 60115, USA
[2]Fermi National Accelerator Laboratory, Batavia, IL 60510, USA

Abstract

A nitrogen gas sheet will measure the two dimensional transverse profile of the 2.5 MeV proton beam in IOTA. The beam lifetime is limited by the interaction with the gas, thus a minimally invasive instrument is required. To produce a gas sheet with the desired density and thickness, various nozzle types are being investigated, including rectangular capillary tubes for gas injection and skimmers for final shaping of the gas. It is essential to meet vacuum requirements in the interaction chamber while maintaining the precise thickness and density of the gas, without significantly affecting the beam lifetime. The current design of a gas sheet beam profile monitor and present status will be discussed.

INTRODUCTION

A minimally invasive gas jet profile monitor is needed to understand correlations of phase-space diffusion with dynamical resonances in a high-intensity beam, space-charge dominated beam. The Integrable Optics Test Accelerator (IOTA) at the Fermilab Accelerator Science and Technology (FAST) Facility supplies a 2.5 MeV proton beam and requires a vacuum pressure of $\sim 10^{-11}$ torr throughout the ring. The pressure in the region in which the gas sheet beam profile monitor will be located can be increased to $\sim 10^{-8}$ torr. Thus, it is crucial to optimize the sheet divergence and gas density. Various nozzle and skimmer configurations for gas injection was simulated, as well as the proton beam and gas interaction.

With a high Knudson number in ultra high vacuum conditions, a molecular flow regime can be assumed. Gas molecules in a reservoir will traverse a nozzle and have a certain distribution entering a lower pressure region. For a cylindrical capillary tube with length l and diameter d, the number of atoms per solid angle exiting can be described by a cosine law distribution [1]:

$$\frac{dN}{d\omega} = p_i \ d^2 \ C_0(l, d, \theta) \ \cos\theta \sqrt{\frac{N_A}{32\pi \ k_B \ M \ T}},$$

where p_i is the partial pressure of the gas species in the reservoir, M is the species molecular weight, N_A is Avogadro's number, and k_B is Boltzmann's constant. $C_0(l, d, \theta)$ is a correction factor, a value between 0 and 1, that depends on whether the molecules escape directly through the capillary

without hitting the wall, and is a function of the dimensions of the capillary. The angle θ is relative to the normal of the orifice. The angular distribution pattern is only dependent on the geometry of the nozzle, i.e. the length and diameter. The exiting gas density is proportional to the reservoir gas density and geometry of the orifice. For a larger length to diameter ratio the exit pattern has a beaming effect as shown in Fig. 1.
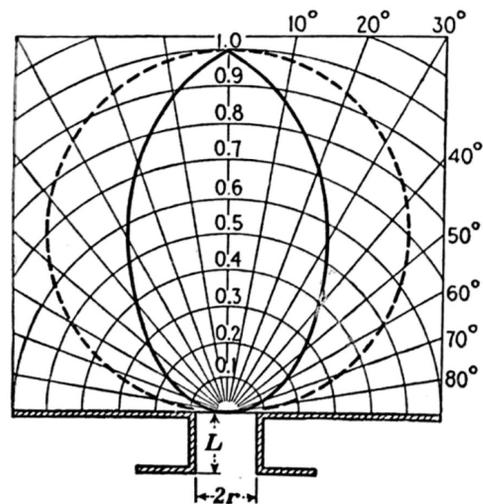

Figure 1: Clausing's diagram of angular distribution for $l/d = 2$ [1].

It is also useful to define the angle at which the distribution falls to half the maximum intensity. This can be represented as [2]:

$$\theta_{\frac{1}{2}} = 0.84\frac{d}{l}. \tag{1}$$

It is assumed that a rectangular capillary can be approximated by a superposition of cylindrical tubes. Thus, the minor axis of the rectangle (i.e. the width), is similar to that of a cylindrical tube diameter, so that the angular distribution will be the same. Therefore a gas sheet of a certain thickness can be formed. A skimmer can be used to select the core of the molecular beam.

SIMULATION OF RECTANGULAR CAPILLARY

The gas sheet system reported in [3], that is to be used in the rapid cycling synchrotron in J-PARC, was modeled and simulated in Molflow+ [4]. The dimensions used at J-PARC and the simulation were: a gas reservoir volume

06 Beam Instrumentation, Controls, Feedback, and Operational Aspects

T03 Beam Diagnostics and Instrumentation

7.5 cm³, a rectangular nozzle $50 \times 0.1 \times 100$ mm (width $\times$ height $\times$ length), and a rectangular skimmer of dimensions $60 \times 0.3 \times 0.5$ mm. The nozzle to skimmer distance at J-PARC was 25 mm, but for the simulation this was varied between 5, 15, and 25 mm. Separately, at a nozzle to skimmer distance of 25 mm, the skimmer was offset on its minor axis by 0.1, 0.5, and 1.0 mm. Detector planes were placed at 0.1 (D1), 10 (D2), 50 (D3), and 100 mm (D4) after the skimmer, along the gas flow direction. The grid size for each detector plane is 100 cells per centimeter.
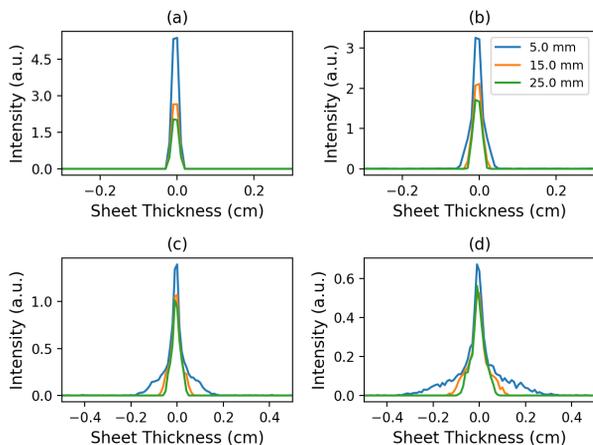

Figure 2: Gas distribution with varying nozzle-skimmer distances.

Figure 2 shows the gas distribution along the minor axis at various nozzle to skimmer distances. Figures 2a, 2b, 2c, and 2d correspond to detector planes at 0.1. 10, 50, and 100 mm, respectively. As the distance between the nozzle and skimmer decreases, the distribution in the tails of the sheet becomes more prominent. However, the density in the core increases.

Table 1: FWHM with Various Nozzle to Skimmer Distances

Distance	D1	D2	D3	D4	Units
5.0	0.22	0.25	0.31	0.42	mm
15.0	0.22	0.27	0.33	0.44	mm
25.0	0.22	0.28	0.33	0.41	mm

Table 1 lists the full width half max (FWHM) of the distribution for each detector plane for varying distances. For each nozzle-to-skimmer distance, the FWHM grew by ~0.2 mm over a span of 100 mm.

Figure 3 shows the gas distribution along the minor axis at various skimmer offsets, with the same detector plane locations as mentioned previously. Somewhere between an offset of 0.1 mm and 0.5 mm the intensity of the sheet drops by an order of magnitude. As can be seen in Fig. 2 and Fig. 3, the intensity of the core decreases with increasing distance from the skimmer.

Table 2 lists the FWHM values for the various nozzle-skimmer offsets. At 50 mm downstream there is a notice-
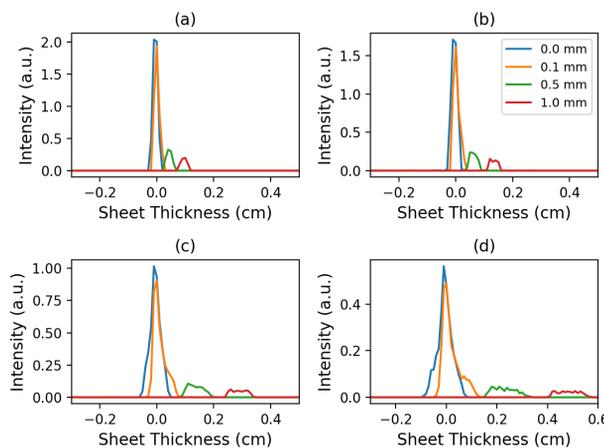

Figure 3: Gas distribution with skimmer offsets.

Table 2: FWHM of Nozzle-Skimmer Offsets

Offset	D1	D2	D3	D4	Units
0.0	0.22	0.28	0.33	0.41	mm
0.1	0.19	0.21	0.28	0.36	mm
0.5	0.27	0.37	0.73	1.19	mm
1.0	0.29	0.38	0.82	1.32	mm

able increase in the FWHM for an offset of 0.5 and 1.0 mm. With no offset and the nozzle-skimmer distance at 25 mm, the FWHM of the sheet measured 100 mm downstream is 0.41 mm. Using the small angle approximation, the divergence of the sheet is ≈ 0.002 radians. Using Eq. (1), the half intensity angle is expected to be ≈ 0.84 mrad. Thus, the expected FWHM at detector plane four is 0.22 mm. This is likely due to the bin size in the simulation or the assumption that a rectangular capillary is a superposition of cylindrical tubes is not entirely valid.

BEAM-GAS INTERACTION

A large effect due to space-charge is expected in IOTA as a result of the beam energy (2.5 MeV) and current (8 mA). Simulations of the beam-gas interaction have been performed using Warp [5], which accurately models the ionization process and space-charge, in an effort to quantify the effect of space-charge as well as extraction electrode strength on the expected signal.

Simulation Parameters

A beam with a Gaussian distribution ($\sigma_{x,y} = 3.5$ mm) was injected. The gas sheet was approximated by 150 containers of nitrogen gas with dimensions 70x0.2x0.2 mm (x,y,z) offset from each other in y and z by 0.2 mm so that a sheet extending ± 1.5 cm in y, rotated by 45° with respect to the z-axis was formed. Four annular electrodes, each with an inner diameter of 2.5 cm, an outer diameter of 3.0 cm, and length of 0.5 cm were placed at y positions of -2.5, 2.5, 3.5, and 4.5 cm, centered in z with the gas sheet. The electrodes

were biased at +500, -500, -1000, and -1500 V from bottom to top in order to direct the plasma ions toward a virtual detector. Figure 4 shows the simulation domain in the y-z plane close to the beginning of the beam pulse. The gas
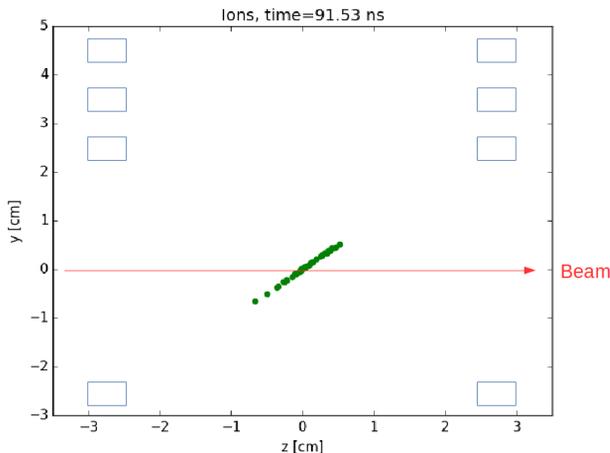

Figure 4: Simulation domain in the y-z plane. The green dots are ion macroparticles generated by the beam (direction shown in red) interacting with the gas (not shown). The cross section of the electrodes are outlined in blue. This snapshot was recorded 91.53 ns into the simulation.

density was set to 4×10^{11} cm^{-3} and the cross section for ionization is 7.19×10^{-17} cm^2.

The distribution of ions was recorded at various y positions extending up to 2.5 cm over the course of the beam pulse (1.77 µs). The distribution in x of the ions should match the distribution in x of the beam, and the distribution in z of the ions should match the distribution in y of the beam, with some smearing coming from the sheet thickness, due to the 45° angle between the beam and the sheet.

Simulation Results

The x and y distributions of the beam are shown in Fig. 5. In all histograms, the bin size corresponds to the simulation grid size -1 mm in x and y, and 0.2 mm in z.
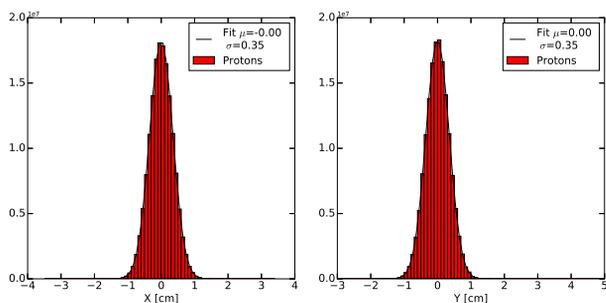

Figure 5: Transverse distributions for the beam (x – left, y – right), with Gaussian fits.

The x and z distributions of all ions that passed through a slice in y between 2.39 and 2.50 cm (chosen based on ion

velocity so that no macroparticles pass through without being counted) are shown in Fig. 6. It can be seen that the
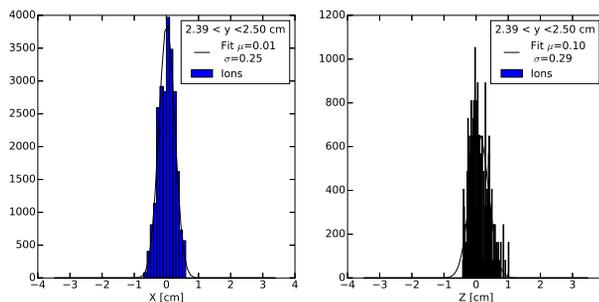

Figure 6: Transverse distributions (x – left, z – right) for all ions to have passed through a slice in y between 2.39 and 2.50 cm over the course of the beam pulse, with Gaussian fits.

width of the distribution of ions does not match in either transverse direction to that of the beam. This is due to both space-charge and the strength of the extraction electrodes. As seen in Fig. 7, the ion distribution more closely matches that of the beam closer to the beam center. Also of note is
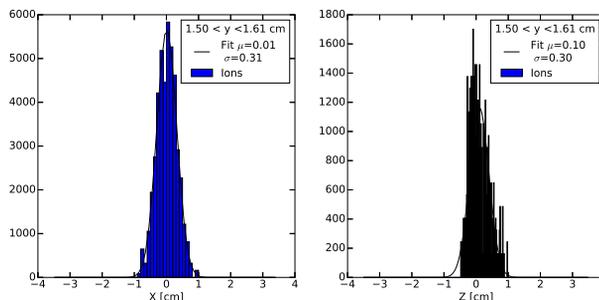

Figure 7: Transverse distributions (x – left, z – right) for all ions to have passed through a slice in y between 1.50 and 1.61 cm over the course of the beam pulse, with Gaussian fits.

that roughly half of all plasma ions created during a single beam passage do not make it to the virtual detector position ($y = 2.5$ cm) during the revolution period of the beam. This indicates a potential issue with detector pileup that will need to be addressed in the readout electronics. Further studies are underway to optimize the strength of the extraction electrodes and quantify the effect of space-charge and electrode strength on the signal distribution.

SUMMARY

Simulations of the beam-gas interaction have been done. MolFlow+ simulations were used to estimate a gas sheet distribution for various configurations of nozzles and skimmers. Construction of a test bench is underway at FAST at Fermilab. This will be used to validate the simulation results for various nozzle and skimmer configurations.

REFERENCES

[1] B. B. Dayton, "Gas Flow Patterns at Entrance and Exit of Cylindrical Tubes", *Trans. 3rd Nat. Vac. Symp.*, pp. 5-11 (1956).

[2] J.A. Giordmaine and T.C. Wang, "Molecular Beam Formation by Long Parallel Tubes", *J. Appl. Phys.*, **31**, pp. 463-471 (1960).

[3] N. Ogiwara *et al.*, "A Non-Destructive Profile Monitor Using a Gas Sheet", in *Proc. IPAC2016*, pp. 2102-2104.

[4] R. Kersevan and M. Ady, "MolFlow+ - A Monte-Carlo Simulator Package Developed at CERN," 2015. `https://molflow.web.cern.ch`

[5] A. Friedman et al., "Computational Methods in the Warp Code Framework for Kinetic Simulations of Particle Beams and Plasmas", *IEEE Trans. Plasma Sci.,* **42**, 5, p. 1321, (2014).